Applied Microbiology and Biotechnology (2023) 107:835–851
https://doi.org/10.1007/s00253-022-12323-0

APPLIED MICROBIAL AND CELL PHYSIOLOGY

Deletion of gene OV132 attenuates Orf virus more effectively than gene OV112

Yumiko Yamada[1] · Shih-Te Chuang[2] · Ching-Yu Tseng[1] · Guan-Ru Liao[1] · Shin-Wu Liu[2] · Yeu-Yang Tseng[3] · Fong-Yuan Lin[4] · Wei-Li Hsu[1]

Received: 8 August 2022 / Revised: 27 November 2022 / Accepted: 30 November 2022 / Published online: 9 December 2022

Abstract

Orf virus (ORFV), a *Parapoxvirus* in *Poxviridae*, infects sheep and goats resulting in contagious pustular dermatitis. ORFV is regarded as a promising viral vector candidate for vaccine development and oncolytic virotherapy. Owing to their potential clinical application, safety concerns have become increasingly important. Deletion of either the OV132 (encoding vascular endothelial growth factor, VEGF) or OV112 (encoding the chemokine binding protein, CBP) genes reduced ORFV infectivity, which has been independently demonstrated in the NZ2 and NZ7 strains, respectively. This study revealed that the VEGF and CBP gene sequences of the local strain (TW/Hoping) shared a similarity of 47.01% with NZ2 and 90.56% with NZ7. Due to the high sequence divergence of these two immunoregulatory genes among orf viral strains, their contribution to the pathogenicity of Taiwanese ORFV isolates was comparatively characterized. Initially, two ORFV recombinants were generated, in which either the VEGF or CBP gene was deleted and replaced with the reporter gene EGFP. In vitro assays indicated that both the VEGF-deletion mutant ORFV-VEGFΔ-EGFP and the CBP deletion mutant ORFV-CBPΔ-EGFP were attenuated in cells. In particular, ORFV-VEGFΔ-EGFP significantly reduced plaque size and virus yield compared to ORFV-CBPΔ-EGFP and the wild-type control. Similarly, in vivo analysis revealed no virus yield in the goat skin biopsy infected by ORFV-VEGFΔ-EGFP, and significantly reduced the virus yield of ORFV-CBPΔ-EGFP relative to the wild-type control. These results confirmed the loss of virulence of both deletion mutants in the Hoping strain, whereas the VEGF-deletion mutant was more attenuated than the CBP deletion strain in both cell and goat models.

Key points

- *VEGF and CBP genes are crucial in ORFV pathogenesis in the TW/Hoping strain*
- *The VEGF-deletion mutant virus was severely attenuated in both cell culture and animal models*
- *Deletion mutant viruses are advantageous vectors for the development of vaccines and therapeutic regimens*

Keywords Parapoxvirus · Chemokine binding protein · Vascular endothelial growth factor · Pathogenesis · Attenuation

Introduction

Orf virus (ORFV), the prototype species of the genus Parapoxvirus within the *Poxviridae* family, causes highly contagious skin lesions, referred to as orf, in several species of small ruminants, particularly sheep and goats. It consists of a double-stranded DNA molecule of roughly 138 kb long (Haig and Mercer 1998). ORFV is a zoonotic pathogen that occasionally infects humans (Haig and Mercer 1998). The disease is typically benign, with lesions that progress through a well-liked stage and create pustules within a few days. Rupture of the pustules results in ulcers and, subsequently, a thick and overlying crust that is shed within 4–6 weeks (Fleming et al. 2017). The mortality rate of

✉ Wei-Li Hsu
wlhsu@dragon.nchu.edu.tw

1 Graduate Institute of Microbiology and Public Health, National Chung Hsing University, Taichung, Taiwan

2 Department of Veterinary Medicine, College of Veterinary Medicine, National Chung Hsing University, Taichung, Taiwan

3 WHO Collaborating Center for Reference and Research On Influenza, Peter Doherty Institute for Infection and Immunity, VIDRL, University of Melbourne, Melbourne, VIC, Australia

4 Department of Animal Healthcare, Hungkuang University, Taichung, Taiwan

ORFV infection can reach up to 10% in lambs and may be as high as 93% in kids (Hosamani et al. 2009). This high mortality in young animals was due to their inability to suck and consume nutrition properly (Hosamani et al. 2009). Wild-type ORFV transmission to adults can occur on scarred skin, but it always remains clinically unapparent, and in exceedingly rare cases, proliferative lesions are seen.

In common with other poxviruses, ORFV expresses a variety of immunomodulatory proteins (IMPs) responsible for regulating the host-innate and pro-inflammatory responses to infection (Weber et al. 2003). For the past years, the function(s) and the underlying mechanism(s) of the ORFV-encoded IMPs had been determined. Examples of these IMPs are a chemokine binding protein (CBP) (Fleming et al. 2017), an interleukin 10 homolog (ORFV127) (Fleming et al. 1997), an inhibitor of granulocyte-monocyte colony-stimulating factor and IL-2 (ORFV117) (Deane et al. 2000), an interferon (IFN)-resistance protein (OV20) (Tseng et al. 2015a), a homolog of vascular endothelial growth factor (VEGF) (Wise et al. 1999), and the immunomodulators of the nuclear factor-kappa (NF-κB) signaling pathway (Martins et al. 2017). Although these genes are mainly non-essential for ORFV replication in vitro, it has been noted that the VEGF, CBP, viral homologs of IL-10 (ORFV127), and NF-κB inhibitor ORFV121 are virulence factors that play a part in ORFV pathogenesis in the natural host (Fleming et al. 2017; Savory et al. 2000).

ORFV has been proposed as an ideal viral vector because of its immunomodulatory and biological properties (Rziha et al. 2000). ORFV possesses several unique qualities that make it suitable for the development of parapoxviruses as vectors for vaccine delivery (Friebe et al. 2011; Reguzova et al. 2020). Some of these features include a safety profile, restricted host range, and "exceptionally strong" induction of inflammation and the innate immune system (Martins et al. 2017). ORFV-based vaccines have provided protection against some viral infections, such as rabbit hemorrhagic disease virus (Rohde et al. 2011), classical swine fever (Voigt et al. 2007), Borna disease virus (Henkel et al. 2005), pseudorabies virus (Fischer et al. 2003), rabies virus (Amann et al. 2013), and influenza A virus (Rohde et al. 2013). The major advantage of using recombinant ORFV for vaccination is based on the fact that ORFV generally elicits only short-lived virus-specific immunity in its natural hosts, allowing frequent reinfection owing to the absence of virus-neutralizing antibodies (Reguzova et al. 2020). This feature allows repeated immunizations using ORFV recombinants to boost humoral immune responses against the inserted antigens.

Recently, several studies have demonstrated the oncolytic properties of ORFV in lung cancer (Rintoul et al. 2012) and colorectal cancer (Chen et al. 2021). Given these circumstances, safety is a priority. Several strategies have been used to ensure the safety of viral vectors. These include the selection of natural strains with lower virulence, development of highly attenuated strains (e.g., ORFV strain D1701) (Reguzova et al. 2020), inactivation of virulence factors such as vascular endothelial growth factor (VEGF) (Savory et al. 2000), and deletion of immunomodulatory viral genes (Fleming et al. 1997). Previous studies revealed that the deletion of either the chemokine binding protein (CBP) (Fleming et al. 2017) or VEGF gene (Savory et al. 2000) in the NZ7 and NZ2 strains, respectively, attenuated ORFV infection and presumably reduced the severity of the disease in the host (i.e., sheep). Although ORFV showed an excellent safety profile as a viral vector, there are still circumstances in which ORFV can impose severe infections in an immunocompromised individual when this virus will be applied for therapeutic purposes.

CBP, approximately 32 kDa, is expressed by the gene OV112 (approximately 861 bp) (Fleming et al. 2017), which is one of the virulence genes that can be detected early after the invasion of host cells by ORFV (Heidarieh et al. 2015). OV112 is located in highly variable terminal regions of the ORFV genome, and a high frequency of sequence variations of the OV112 gene has been noted among different strains (Heidarieh et al. 2015). For instance, the sequence of the ORFV NZ7 gene is 27 bp longer than that of its NZ2 counterpart. Moreover, sequence alignment with the NZ2 strain revealed three insertions in NZ7, and the amino acid identity of the CBP of NZ2 and NZ7 strains was only 78% (Seet et al. 2003). ORFV-CBP permits transient expression of the virus antigen in infected cells impeding the reactivation of cytokines and chemokines (McGuire et al. 2012). In addition, the recruitment and migration of dendritic cells and other immune cells to peripheral lymph nodes to activate an adaptive immune response are inhibited by the CBP of ORFV (Chen et al. 2020). Notably, viral CBP have no mammalian homologs (Lateef et al. 2010). In addition, the lack of regulation of immune cells can cause inhibition of the MHC class II pathway, affecting the recruitment and/or activation of cytotoxic T cells at the site of skin infection (Chen et al. 2020).

The viral VEGF protein is encoded by the OV132 gene (~462 bp), an early gene that is located in highly variable terminal regions at the right end of the conserved region of the ORFV genome (Tan et al. 2009). Genetic analysis showed that the ORFV OV132 gene was likely purloined from host organisms during evolutionary coexistence (Lyttle et al. 1994). Substantial sequence variations in VEGF genes between viral strains have been reported (Mercer et al. 2002). For instance, the amino acid sequences of the VEGF gene between the two New Zealand isolates, namely the OV NZ2 and NZ7 strains, showed only 41.1% identity, and surprisingly, little homology at the DNA level was found between the strains (Lyttle et al. 1994). Moreover, viral VEGF is characterized only in the

genus *Parapoxvirus* of *Poxviridea*. Hence, it was postulated that these two ORFV strains acquired the VEGF gene by independent events and from different sources (Lyttle et al. 1994).

Viral VEGF is homologous to mammals and is one of the immunomodulatory proteins responsible for inhibiting the proliferation of host immunity (Wise et al. 1999). However, cellular VEGF is a regulatory protein actively involved in the elimination of tumors (Nash et al. 2006) and virus-infected cells (Achen et al. 1998), as well as in promoting the wound healing process (Shen Ni et al. 2013). A previous study suggested that ORFV-VEGF may stimulate the proliferation of epithelial cells which would enhance the formation of more viral and receptor binding sites for ORFV replication (Wise et al. 1999). In addition to viral replication, ORFV-VEGF protects the virus from the overall effects of immune responses and weakens the host antiviral response (Haig and McInnes 2002). This implies that ORFV-VEGF is responsible for promoting the intracellular replication of the virus by sabotaging the apoptotic activity of the host cell (Wise et al. 1999).

ORFV has emerged as an attractive vector candidate for vaccine development and has potential clinical applications in humans. To this end, the attenuation of ORFV is essential. As mentioned above, sequences of the two virulence determinants (i.e., CBP and VEGF) were substantial variables between viral strains, even for those isolated from the same countries. Moreover, the degree of attenuation between these two deletion ORFVs on their natural host was examined using different experimental designs and evaluation parameters. Hence, the current study aimed to comprehensively characterize the two recombinant ORFVs of the Hoping strain (isolated from Taiwan) with deletions of either the VEGF (OV132) or CBP (OV112) gene. To this end, the infection profile of these single gene-knockout viruses and also their clinical pathology in a natural host were comparatively analyzed in parallel with the ORFV containing wild-type genome. These results demonstrated that recombinant ORFV defective in either VEGF or CBP expression significantly reduced viral infection. Notably, compared with the CBP-null mutant virus, knockout of VEGF expression resulted in severe attenuation of ORFV infectivity in both cell culture and animal models.

Materials and methods

Cell maintenance

Human embryonic kidney cell line 293 T and goat fibroblast (abbreviated as FB) cells were cultured in Dulbecco's modified Eagle's medium (DMEM; Gibco BRL, Life Technologies Corporation, Carlsbad, CA, USA) supplemented with 10% fetal bovine serum (FBS) (GIBCO, Carlsbad USA, CA) and 1% penicillin–streptomycin (Gibco BRL). Cells were cultured at 37 °C and 5% CO_2.

Viruses and infection

The ORFV-WT-EGFP (Hoping strain) was propagated in goat fibroblast cells (FB) as described previously (Lin et al. 2015). For infection, 80% confluent cell monolayers were incubated with ORFV at the indicated multiplicity of infection (MOI) in the infection medium (DMEM without FBS). After allowing 1 h for viral adsorption, the infection medium was replaced with fresh DMEM containing 2% FBS, and the vessels were returned to 37 °C with 5% FBS.

Construction of transfer vectors for generation of recombinant ORFVs

Two transfer vectors were constructed to prepare attenuated viruses. First, the transfer vector (pVEGF$^{\Delta}$-vvTK-eGFP) for ORFV with deletion of the VEGF gene was generated in several steps. Initially, a plasmid harboring flanking (upstream and downstream) sequences of OV132 was generated. DNA fragments containing downstream (namely, OV133) and upstream (i.e., OV131) sequences were amplified from ORFV genomic DNA by PCR with two primer sets comprising built-in restriction enzyme sequences, namely down-VEGF-*Bam*H I-F/down-VEGF-*Eco*R I -R and up-VEGF-*Hind* III-F/up-VEGF-*Xho* I-R, respectively. To generate viruses with a screening marker (EGFP), the two ORFV DNA fragments trimmed with restriction enzymes were individually cloned upstream or downstream of the EGFP coding sequences in the pUC19-H5-EGFP plasmid (Tseng et al. 2015b) and linearized with enzymes compatible with the insert DNA fragments. The resulting plasmid was designated pUC19-VEGF-flanking. To equip recombinant ORFV with a selection marker, the thymidine kinase (vvTK) gene (554 bp) was amplified from the vaccinia virus using the primers vvTK-*Nco* I-F/vvTK-*Bam*H I-R and further inserted into the slp-pETDuet plasmid. Subsequently, vvTK fused with poxvirus late promoter sequences (sLp) was generated by PCR using the primers slp-vvTK-*Xba* I-F and vvTK-*Xba* I-R, and the resulting amplicon (sLp-vvTK, 648 bp) was cloned into a pUC19-VEGF-flanking plasmid.

Using a similar strategy, another transfer vector (pCBP$^{\Delta}$-EGFP) was created. In brief, two fragments containing the right and left flanking sequences of the CBP gene (OV112) were placed upstream, or downstream of the EGFP coding sequences in the vector pUC19- H5-EGFP (Tseng et al. 2015b). Specifically, a fragment that spans 522 bp upstream of the CBP coding region was amplified by PCR using the primer set OV112-up-EcoRI-F/OV112-up-BamHI-R and cloned into the *Eco*R I and *Bam*H I restriction sites of pUC19- H5-EGFP to generate

the pUC19-H5-EGFP-upstream plasmid. Another fragment that spans 560 bp downstream of the CBP coding region was amplified using two primers, OV112-down-XhoI-F and OV112-down-HindIII-R, and then cloned into the vector pUC19-H5-EGFP-upstream at the *Xho* I and *Hin*d III restriction sites. The final plasmid construct is referred to as pCBP$^{\Delta}$-EGFP.

All primers used to amplify the ORFV gene were designed based on ORFV sequences published in GenBank (accession number AY386264.1), and are summarized in Table 1.

Generation of single-gene deletion orf viruses

Recombinant ORFV-VEGF$^{\Delta}$-EGFP and ORFV-CBP$^{\Delta}$-EGFP viruses were generated using a procedure adapted from the standard protocols used in the generation of vaccinia virus recombinants and previously described methods (Byrd and Hruby 2004; Marzook and Newsome 2019; Tseng et al. 2015b; Wyatt et al. 2017). HEK293T cells were infected with wild-type orf virus at an MOI of 0.05. At 1 hpi, infected cells were transfected with one of the transfer vectors, pVEGF$^{\Delta}$-vvTK-eGFP and pCBP$^{\Delta}$-EGFP, specific for generating recombinant orf viruses, ORFV-VEGF$^{\Delta}$-EGFP and ORFV-CBP$^{\Delta}$-EGFP with deletions of VEGF or CBP, respectively. Transfection was performed using Lipofectamine 2000 (Invitrogen, Thermo Fisher Scientific, Carlsbad, CA, USA) following the manufacturer's instructions. Briefly, 3 µL of Lipofectamine 2000 per 1 µg of transfer vector was mixed, incubated at room temperature for 15 min, and added to the cells. After 6 h at 37 °C, the medium containing the transfection mix was removed and replaced with a complete growth medium (DMEM supplemented with 10% FBS). The recombinant virus was monitored for EGFP expression and collected 24–48 h after transfection by scraping cells off the plates and mixing them along with any floating cells in the

Table 1 Primer sequences used in this study

Primer name	Sequence (5′–3′)
Up-VEGF-Hind III-F	ATAAGCTTGACCCCAGAGGCCGCCGACTG
Up-VEGF-Xho I-F	TTTCTCGAGCTCAAAGCCTATCCAGACAC
Down-VEGF-EcoR I-R	CCGAATTCCGGTCACAATGTCGTATGAGGTG
Down-VEGF-BamH I-R	TTTGGATCCGTCTGGGCACGCAATTTATT
slp-vvTK-Xba I-F	GGATAACAATTCCCCTCTAGATTTTTTT
vvTK-Xba I-R	GGGGTCTAGATTATGAGTCGATGTAACACTTTCTAC
vvTK-Nco l-F	TTTCCATGGATGAACGGCGGACATATTC
vvTK-BamH l-R	GGGGGGATCCTTATGAGTCGATGTAACACTTTCTAC
rVEGF-BamH I-F	GGGGATCCTTCTGTTAATGAATGGATGCAAACATTAGG
rVEGF-Xho I-F	GGGCTCGAGAACGACTACGGTTGTATTTCTTGTT
VEGF-F	CCAGAATGCGTGTCTCAGGG
VEGF-R	GTTACAGCAACCACTGCATCG
eGFP-F	AAGGATCCATGGTGAGCAAGGGCGAG
eGFP-R	TTGTCGACTTACTTGTACAGCTCGTCC
OV112-up-EcoRI-F	GAATTCCCCGGCGACGGAGATCTC
OV112-up-BamHI-R	ATTTATTGGATCCCCTGATTGTTGCAAGATTCCAGAG
OV112-down-XhoI-F	CTCGAGGATGTTTTTATTCGGCAATATAATAGGTG
OV112-down-HindIII-R	AAGCTTCCAGGCCCCACCTCCAC
OV112-F	ATGAAGGCGNTGGTGTTG
OV112-R	ATGGCCAGGGCTGAGGTTAAG
OV111-F	ATTCGGCGACATGCTGTACGC
OV113-R	CCCCACTTCCACCTCTACCTC
OV112-F1-F	GGGGCATATGAAGGCGGTGGTGTTGTTG
OV112-F1-R	GGCTCGAGATCCATTACGGAGTCTTC
OV112-F2-F	GGCATATGGATAATGAATACATGTCTGCG
OV112-F2-R	GGGCTCGAGGTTCGCAGATAAGTCCTG
OV112-F3-F	TTTCATATGGCGAACGGCAGCTGGG
OV112-F3-R	GGGCTCGAGCTTTCTGTTTACACTGGCG
OV112-F4-F	GGGGCATATGAAGGCGGTGGTGTTGTTG
OV112-F4-R	GGCTCGAGATCCATTACGGAGTCTTC

The underlined primer sequences highlight the restriction enzyme recognition sites

culture followed by sonication. The cell lysate containing the orf virus was tenfold serially diluted and inoculated into the FB cells. The infected cell monolayer was overlaid with 1.2% methyl cellulose, and cell morphology was observed daily by fluorescence microscopy. Individual fluorescing plaques were selected and subjected to several rounds of plaque purification.

The total genomic DNA isolated from the recombinants per round of plaque purification was characterized using restriction endonuclease, PCR, and western blot analyses.

Genotyping of single-gene deletion orf viruses

The genotypes of the two recombinant viruses were validated using PCR. To confirm the deletion of the target gene, PCR with the primer set VEGF-F/VEGF-R or OV112-F/OV112-R was used to amplify VEGF and CBP, respectively, from the viral genome. Moreover, the presence of the inserted gene cassette in the ORFV-VEGF$^{\Delta}$-EGFP virus, including vvTK and EGFP, was further validated by PCR with the primer set vvTK-Nco l-F/vvTK-Xba I-R or eGFP-F/eGFP-R, respectively.

Additionally, restriction fragment length polymorphism (RFLP) analysis was conducted to confirm the ORFV-CBP$^{\Delta}$-EGFP genotype. To do so, a fragment spanning two open reading frames adjacent to OV 112 was amplified by PCR using primers OV111-F and OV113-R. Subsequently, ORFV-CBP$^{\Delta}$-EGFP and ORFV-WT-ORFV (2095 bp and 2024 bp, respectively) were reacted with a restriction enzyme, either *Bgl* II or *Nco* I. The RFLP pattern of ORFV-CBP$^{\Delta}$-EGFP was comparatively analyzed with that of ORFV-WT-ORFV. The primers used for genotyping are listed in Table 1.

Preparation of anti-serum for ORFV-VEGF and CBP

To confirm the deletion of the target genes, two antibodies against ORFV-VEGF and CBP proteins were generated to detect target gene expression. First, an immunogen is produced in prokaryotic cells. The VEGF gene was amplified from wild-type ORFV DNA by PCR using primers rVEGF-*Bam*H I-F and rVEGF-*Xho* I-R. The PCR product was trimmed by *Bam*H I and *Xho* I and cloned into pET32b linearized with the corresponding enzymes. Recombinant CBP was expressed in four fragments to increase the yield. The four fragments (OV112-F1 to -F4) with expected sizes of 224 bp, 228 bp, 224 bp, and 220 bp, which covered the whole region of the CBP protein, were individually amplified by PCR with primer sets (OV112-F1-F/OV112-F1-R ~ OV112-F4-F/OV112-F4-R, Table 1). Subsequently, the four amplicons were reacted with *Nde* I and *Xho* I enzymes and ligated with pET24a vectors linearized with compatible enzymes. Expression and purification of recombinant proteins (rVEGF, CBP F1-F4 fragments) followed the protocol established in our laboratory (Tseng et al. 2015b). Production of polyclonal anti-serum for VEGF and CBP was carried out by Yao-Hong Biotechnology, Inc. (Taipei, Taiwan).

Analysis of sequence variations and phylogenetic relationships

The chemokine binding protein and vascular endothelial growth factor protein sequences of orf virus reference strains isolated from different countries were downloaded from the NCBI GenBank database. To perform a comparative analysis of the sequences, related protein sequences were aligned using the CLUSTAL W multiple sequence alignment program, version 1.83, MegAlign module of Lasergene DNA Star software Pairwise.

The accession numbers of all the reference strains used in this study are summarized in Table 2.

Western blot analysis

Proteins were resolved by sodium dodecyl sulfate–polyacrylamide gel electrophoresis (SDS-PAGE) and then electrophoretically transferred to a polyvinylidene difluoride (PVDF) membrane, followed by immunoblotting with diluted antibodies against viral proteins, F1L and VEGF (1:2500, homemade), EGFP (homemade 1:2000), and alpha-tubulin (Novusbio, 1:10,000) overnight at 4 °C. Goat anti-mouse or rabbit IgG conjugated with horseradish peroxidase (HRP) were used as secondary antibodies and incubated with the membrane for 1 h at room temperature. After the membrane was washed with 0.05% Tween 20 in PBS, the signal was detected using an enzyme-linked chemiluminescence assay (SuperSignal; Thermo Scientific). Images were captured using ImageQuant LAS 4000 (GE Healthcare, Uppsala, Sweden), and the intensity of each band was determined by densitometry (ImageJ, NIH).

Plaque assay

FB cells were seeded one night before infection and infected with tenfold serially diluted viruses. One hour post-adsorption, the infectious medium was replaced with 1.1% methylcellulose in DMEM with 2.5% FBS. Infection was monitored daily until a cytopathic effect (CPE) was observed (~ 14 days). The cells were fixed with 10% formaldehyde and stained with crystal violet.

Viral infection of goats

All animal experiments described in this study were approved by the National Chung Hsing University (NCHU)

Table 2 Accession numbers of reference sequences

Name	Gene	Accession no	Ref. no
TW/Hoping strain	CBP	OP056416	–
D1701	CBP	HM133903	(McGuire et al. 2012)
NZ7	CBP	AAR18811	(Seet et al. 2003)
NZ2	CBP	ABA00630	(Mercer et al. 2006)
Bangalore/89/05/Goat	CBP	AWN09366	–
Hubei/2013	CBP	AHJ61508	–
Malaysia/goat/2020	CBP	UAJ23439	–
Ludhiana/50/Goat/2006	CBP	AWN09367	–
Hyderabad/25/Sheep/2006	CBP	AWN09365	–
Gujarat/SP26/Goat/2006	CBP	AWN09364	–
Alwar/Goat/2008	CBP	AWN09363	–
Shahjahanpur/82/Goat/2004	CBP	AWN09360	–
PVNZ	CBP	QDO67043	(Sharif et al. 2019)
BPSV	CBP	AIY25487	–
Human VEGF-A	VEGF	NG_008732	(Eswarappa et al. 2014)
HLJ05	VEGF	MK317956	–
VEGF-D	VEGF	JN603825	(de Castro et al. 2022)
D1701	VEGF	HM133903	(McGuire et al. 2012)
ITC2	VEGF	DQ012965.1	(Mercer et al. 2002)
ITTo	VEGF	DQ012964	(Mercer et al. 2002)
NA1-11	VEGF	KF234407	–
NA17	VEGF	MG674916	–
NP	VEGF	KP010355	(Chi et al. 2015)
NZ2	VEGF	DQ184476	(Mercer et al. 2006)
HN3-12	VEGF	KY053526	–
IA82	VEGF	AY386263	(Delhon et al. 2004)
SJ1	VEGF	KP010356	(Chi et al. 2015)
Pseudocowpox	VEGF	GQ329669	(Hautaniemi et al. 2010)
TW/Hoping strain	VEGF	OP056415	–
NZ7	VEGF	S67522	(Lyttle et al. 1994)

Animal Ethics Committee (IACUC No. 110–106). Animals were housed in an ABSL-2 facility at the Research Center for Animal Medicine, NCHU, Taiwan. The experiment design followed the method from Mercer's laboratory (Fleming et al. 2017). Briefly, three 8-month-old Nubian goats, representing three repeats, were individually inoculated with one of the three orf viruses (ORFV-VEGF$^{\Delta}$-EGFP, ORFV-CBP$^{\Delta}$-EGFP, and ORFV-WT-EGFP) on the epidermis of each leg. An approximately 3-cm-long scratch was made in the skin of the legs using a bifurcated needle and infected by topical application of 100 µL of virus (10^6 pfu) or PBS only (no virus control). Virus-induced lesions were photographed daily for 10 days, and clinical scores were determined. The goats were examined for erythema, papule formation, pustule formation, and firmly attached scabs associated with scarified/infected areas of the skin. The clinical scores were determined by counting the discrete round raised papules with a creamy appearance that formed on the skin surface along the lines of scarification using magnified photographic images and the width of the lesions (1–10 mm) that formed when papules coalesced (days 5–7). Clinical scores ranged from 0 to 3 (0, "no clinical sign of inflammation nor papule on the skin"; 1, "mild to moderate inflammation and visible slight papule"; 2, "moderate to severe papule and mild vesicular"; and 3, "moderate to severe vesicular and moderate pustular to severe pustular"). The clinical scores utilized in this study were determined as per the pathogenesis of ORFV infection recommended by a qualified and experienced veterinarian. The clinical scores for all animals at all time points were determined by two qualified and experienced veterinarians.

Punch biopsies (3 mm) were performed on days 4, 7, and 10 post-infection. Blood samples were collected from the jugular vein of each animal before infection. The viral loads in the lesion were measured using a standard plaque assay or reverse transcription-polymerase chain reaction (RT-PCR).

Histology examination of goat skin by hematoxylin and eosin (H&E) staining

Skin biopsies (3 mm) from goats were fixed with 10% formalin and embedded in paraffin wax. Sections were cut at 4 µm, mounted on glass slides, and stained with H&E, as described by Feldman and Wolfe (2014).

Statistical analysis

Data are expressed as mean ± standard deviation. Student's *t* test was used to determine significant differences. Statistical analysis was performed using GraphPad Prism version 8.00 (GraphPad Software). Statistical significance was set at $p < 0.05$ and is represented by the asterisk sign (*, **, and *** indicate p values < 0.05, 0.01, and 0.001, respectively).

Results

Sequence analysis of OV132 and OV112 of ORFV (Hoping strain)

Based on previous reports, sequences of ORFV genes encoding VEGF (OV132) and CBP (OV112) were highly variable, especially the OV132 gene. Hence, initially, the region consisting of the coding sequence as well as the flanking regions adjacent to the target gene of our local strain (TW/Hoping) was determined. Sequence analysis indicated that VEGF of the Hoping strain was phylogenetically close to NZ7 and distant from NZ2 (Figure S1). Overall, there was an approximately 9% sequence divergence in both genes between the TW/Hoping and NZ7 strains. Specifically, alignment of the nucleotide sequence indicated the OV132 gene of TW/Hoping shares 90.17% similarity with that of NZ7 and as low as 47.01% with that of NZ2 (Fig. 1A). NZ2 and NZ7 are the two model strains commonly used for the study of ORFV pathogenicity in goat models (Fleming et al. 2017; Savory et al. 2000). Compared with VEGF, a higher similarity was noticed in the OV112 gene that encodes CBP among different strains; as shown in Fig. 1B, there is approximately 90–91% of similarity between the Taiwanese (TW/Hoping) strain and the two model strains (Fig. 1B).

Generation of recombinant orf viruses with deletion of the OV132 or OV112 gene

Considering the high sequence variation between the NZ2 and NZ7 strains, it is important to evaluate the role of the

A. OV132 (VEGF)

Identity (%) / Divergence

	1	2	3	4	5	6	7	8	9	10	11	12	13	14	15	16	
1		32.48	34.19	36.75	36.32	36.32	35.47	32.91	32.48	34.19	35.47	35.04	32.91	35.04	31.20	31.62	1.Human VEGF-A
2	67.52		49.15	37.61	48.72	48.72	48.72	99.57	84.19	49.57	48.72	47.86	94.87	66.67	91.88	93.16	2. HLJ05
3	65.81	50.85		44.02	97.44	97.44	97.01	48.72	49.57	99.57	97.01	95.30	49.15	42.74	46.58	46.15	3. VEGF-D
4	63.25	62.39	55.98		44.44	44.44	44.87	37.18	37.18	43.59	44.87	45.30	38.03	37.61	37.61	35.90	4. D1701
5	63.68	51.28	2.56	55.56		100.00	97.01	48.29	49.15	97.01	97.01	94.44	48.72	41.03	46.15	45.73	5. ITC2
6	63.68	51.28	2.56	55.56	0.00		97.01	48.29	49.15	97.01	97.01	94.44	48.72	41.03	46.15	45.73	6. ITTo
7	64.53	51.28	2.99	55.13	2.99	2.99		48.29	48.29	96.58	100.00	94.87	48.72	41.45	45.73	45.73	7. NA1-11
8	67.09	0.43	51.28	62.82	51.71	51.71	51.71		84.19	49.15	48.29	47.44	95.30	66.67	92.31	93.16	8. NA17
9	67.52	15.81	50.43	62.82	50.85	50.85	51.71	15.81		50.00	48.29	47.86	85.47	69.23	88.46	81.20	9. NP
10	65.81	50.43	0.43	56.41	2.99	2.99	3.42	50.85	50.00		96.58	94.87	49.57	42.31	47.01	46.58	10. NZ2
11	64.53	51.28	2.99	55.13	2.99	2.99	0.00	51.71	51.71	3.42		94.87	48.72	41.45	45.73	45.73	11. HN3-12
12	64.96	52.14	4.70	54.70	5.56	5.56	5.13	52.56	52.14	5.13	5.13		47.86	42.74	45.30	44.44	12. IA82
13	67.09	5.13	50.85	61.97	51.28	51.28	51.28	4.70	14.53	50.43	51.28	52.14		64.96	91.03	91.88	13. SJ1
14	64.96	33.33	57.27	62.39	58.97	58.97	58.55	33.33	30.77	57.69	58.55	57.27	35.04		67.95	67.52	14. Pseudocowpox
15	68.80	8.12	53.42	62.39	53.85	53.85	54.27	7.69	11.54	52.99	54.27	54.70	8.97	32.05		90.17	15. TW/Hoping
16	68.38	6.84	53.85	64.10	54.27	54.27	54.27	6.84	18.80	53.42	54.27	55.56	8.12	32.48	9.83		16. NZ7

B. OV112 (CBP)

Identity (%) / Divergence

	1	2	3	4	5	6	7	8	9	10	11	12	
1		91.23	90.89	91.23	93.76	91.06	90.89	90.89	91.23	91.06	90.73	90.22	1. TW/Hoping
2	8.77		95.28	91.40	91.23	90.89	89.88	89.38	90.89	90.56	90.39	90.39	2. D1701
3	9.11	4.72		91.40	90.89	91.40	90.22	89.54	91.06	90.89	91.06	90.56	3. NZ7
4	8.77	8.60	8.60		92.24	90.89	89.54	88.87	90.89	90.22	90.73	90.39	4. NZ2
5	6.24	8.77	9.11	7.76		90.73	90.39	89.88	90.73	91.23	91.06	90.22	5. Bangalore/89/05/Goat
6	8.94	9.11	8.60	9.11	9.27		93.25	93.09	97.98	96.80	97.30	97.13	6. Hubei/2013
7	9.11	10.12	9.78	10.46	9.61	6.75		97.81	93.42	92.92	93.59	93.59	7. Malaysia/goat/2020
8	9.11	10.62	10.46	11.13	10.12	6.91	2.19		93.42	92.58	93.76	93.42	8. Ludhiana/50/Goat/2006
9	8.77	9.11	8.94	9.11	9.27	2.02	6.58	6.58		96.46	97.30	98.82	9. Hyderabad/25/Sheep/2006
10	8.94	9.44	9.11	9.78	8.77	3.20	7.08	7.42	3.54		96.80	96.63	10. Gujarat/SP26/Goat/2006
11	9.27	9.61	8.94	9.27	8.94	2.70	6.41	6.24	2.70	3.20		96.80	11. Alwar/Goat/2008
12	9.78	9.61	9.44	9.61	9.78	2.87	6.41	6.58	1.18	3.37	3.20		12. Shahjahanpur/82/Goat/2004

Fig. 1 Sequence analysis of orf viruses. Sequence similarity in the OV132 (**A**) and OV112 (**B**) genes and various ORFV strains isolated from different countries were analyzed using the CLUSTAL W multiple sequence alignment program, version 1.83, of the MegAlign module of Lasergene DNA Star software Pairwise. The strains analyzed in this assay are summarized in Table 2

two virulence factors involved in the TW/Hoping strain. To generate traceable ORFV, the enhanced green fluorescent protein (EGFP) reporter gene was inserted into the genome of ORFV (Hoping strain) to replace the entire coding region of the virulence genes, that is, either VEGF (Fig. 2A) or CBP (Fig. 3A), by means of homologous recombination. Moreover, the thymidine kinase (vvtk) gene of the vaccinia virus was inserted into the genome of the VEGF-deletion virus, which could serve as a selection marker for the subsequent run of recombinant virus manipulation (Lye and Wang 1996). After several rounds of plaque purification, viral DNA was extracted to confirm the genotype of these recombinant ORFVs, in comparison with that of ORFV-WT-EGFP, another reporter virus consisting of the EGFP gene inserted between the OV20 and OV21 loci of the wild-type viral genome that was previously established (Tseng et al. 2015b).

As indicated in Fig. 2B, the OV132 gene was deleted from the ORFV-VEGF$^{\Delta}$-EGFP genome. Moreover, fragments with the expected molecular weights of vvTK and EGFP were successfully amplified by PCR with gene-specific primers from the recombinant ORFV (Fig. 2C). Notably, the plaque size of ORFV-VEGF$^{\Delta}$-EGFP was smaller than that of ORFV-WT-EGFP, as visualized by the

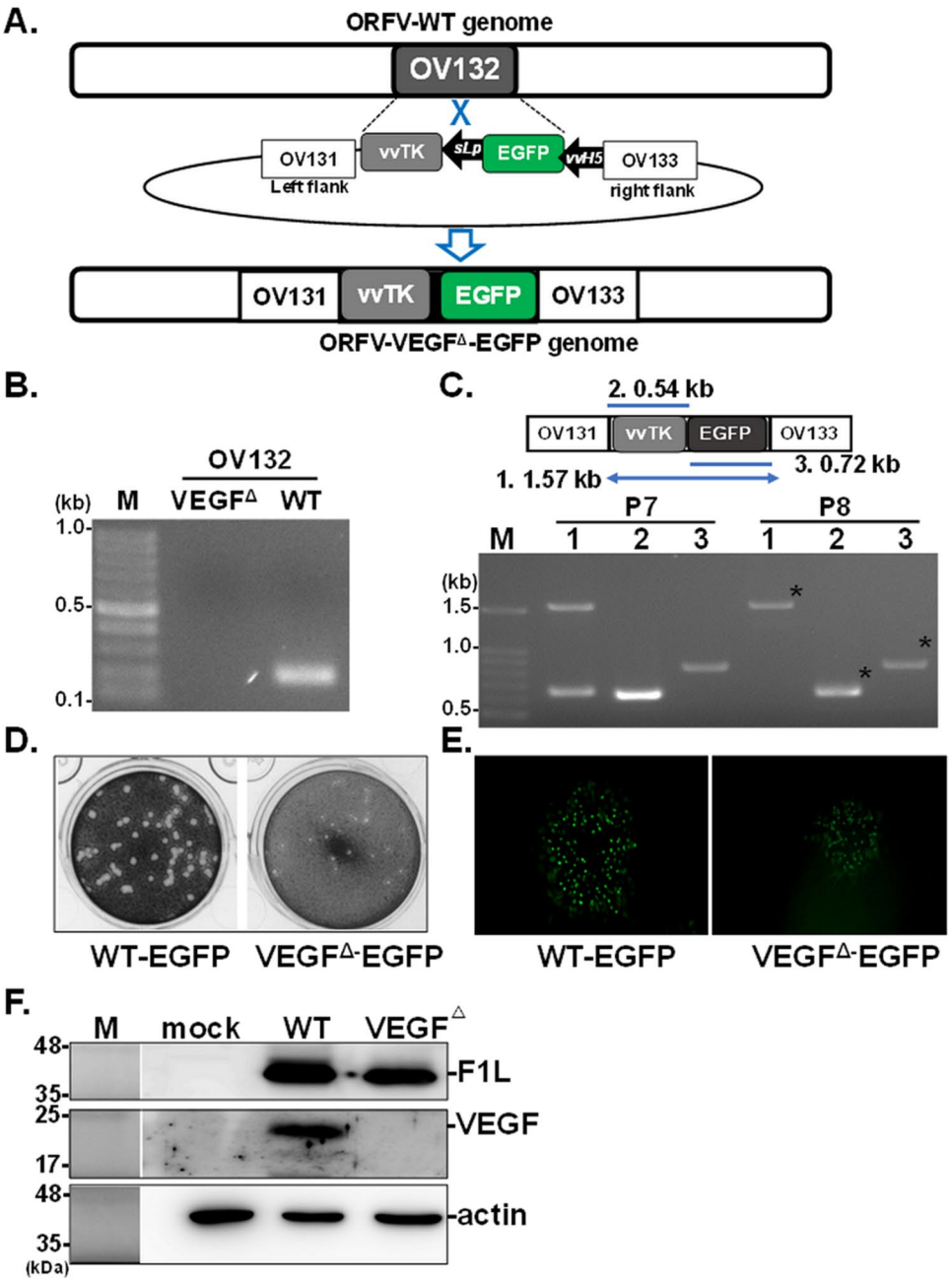

Fig. 2 Generation and validation of recombinant ORFV with VEGF deletion. **A** Schematic representation of ORFV genomes and the expression cassette of the transfer vector for generation of VEGF-null mutant virus by homologous recombination between transfer vector DNA and the ORFV genome (Hoping strain). The genotype of the ORFV-VEGF$^{\Delta}$-EGFP virus was confirmed by the absence of OV132 (**B**) and the insertion of both vvTK and EGFP fragments (**C**) by PCR. Representative results demonstrating the deletion of OV132 (**B**) and the presence of vvTK and EGFP (**C**) in the genome of the ORFV-VEGF$^{\Delta}$-EGFP virus. The plaque of ORFV-VEGF$^{\Delta}$-EGFP was visualized using Giemsa staining (**D**) or direct fluorescent microscopy (**E**). The ORFV-VEGF$^{\Delta}$-EGFP virus that failed to express VEGF was validated by western blot analysis using an antibody specific for VEGF (**F**). F1L and actin served as quality controls for ORFV infection and cell condition, respectively. The viruses with wild-type genome, including parental WT virus (WT) or the one with insertion of a reporter gene (WT-EGFP), served as a control for genotyping and also for monitoring infection in panels **B** and **C** and **D**–**F**, respectively

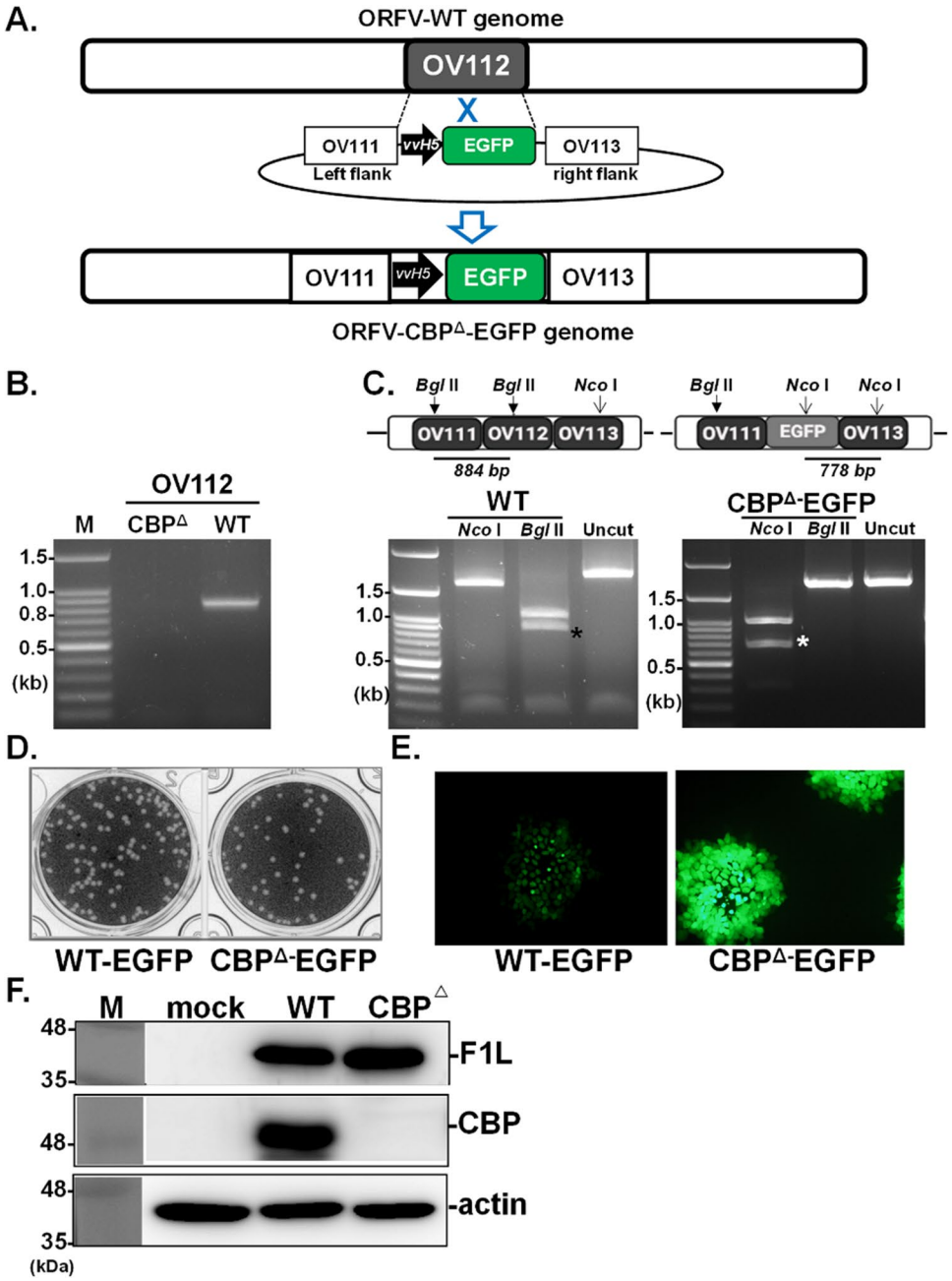

Fig. 3 Generation and validation of recombinant ORFV with CBP deletion. **A** Schematic representation of ORFV genomes and the expression cassette of the transfer vector for generation of CBP-null mutant virus by homologous recombination between transfer vector DNA and the ORFV genome (Hoping strain). The genotype of the ORFV-CBP$^{\Delta}$-EGFP virus was confirmed by the absence of OV112 using PCR amplification (**B**). The identity and purity of the recombinant ORFV-CBP$^{\Delta}$-EGFP genome was validated using the RFLP-PCR profile (**C**). The plaque of ORFV-CBP$^{\Delta}$-EGFP was visualized using Giemsa staining (**D**) or direct fluorescent microscopy (**E**). The ORFV-CBP$^{\Delta}$-EGFP virus that failed to express CBP was validated by western blot analysis using an antibody specific for CBP (**F**). F1L and actin served as quality controls for ORFV infection and cell condition, respectively. The viruses with wild-type genome, including parental WT virus (WT) or the one with insertion of a reporter gene (WT-EGFP), served as a control for genotyping and also for monitoring infection in panels **B** and **C** and **D**–**F**, respectively

standard plaque assay (Fig. 2D) and fluorescence microscopy (Fig. 2E).

The ORFV-CBP$^{\Delta}$-EGFP virus was validated using strategies similar to those for the ORFV-VEGF$^{\Delta}$-EGFP virus. First, the OV112 was absent from the ORFV-CBP$^{\Delta}$-EGFP genome (lane CBP$^{\Delta}$ in Fig. 3B). Moreover, since OV112 contains *Bgl* II, while EGFP has *Nco* I, replacement of the OV112 gene by insertion of the EGFP cassette altered the cutting pattern of the restriction enzyme. Hence, the identity and purity of the recombinant virus were confirmed by restriction fragment length polymorphism (RFLP). A fragment spanning OV111 to OV113 was amplified from the viral genome followed by digestion with either *Bgl* II or *Nco* I enzyme. As illustrated in Fig. 3C, compared with ORFV-WT-EGFP, the recombinant virus ORFV-CBP$^{\Delta}$-EGFP contains one additional *Nco* I site; therefore, *Nco* I digestion yielded two major fragments of 1233 bp and 778 bp, while there was only one major fragment observed in the wild-type virus. On the other hand, due to the presence of additional *Bgl* II sites in the wild-type viral genome, the reaction of this enzyme produced two fragments (1142 bp and 884 bp), which is distinct from the ORFV-CBP$^{\Delta}$-EGFP virus

(Fig. 3C). Notably, unlike the ORFV-VEGF$^{\Delta}$-EGFP virus, the plaque size of the ORFV-CBP$^{\Delta}$-EGFP virus was similar to that of ORFV-WT-EGFP (Fig. 3D), and the expression of EGFP was stronger than that of ORFV-WT-EGFP (Fig. 3E). Among the three viruses, ORFV-VEGF$^{\Delta}$-EGFP demonstrated the weakest EGFP signal, whereas the ORFV-CBP$^{\Delta}$-EGFP virus showed the strongest EGFP expression.

Importantly, in addition to reporter gene expression, knockout of VEGF or CBP expression from recombinant viruses was confirmed. As shown in Figs. 2F and 3F, both viruses encoded the viral F1L protein, while VEGF and CBP proteins were not detected in ORFV-VEGF$^{\Delta}$-EGFP or ORFV-CBP$^{\Delta}$-EGFP viruses, respectively. Taken together, these data indicate the successful generation of recombinant orf viruses with deletion of either the VEGF or CBP genes.

Characterization of the recombinant ORFV in vitro

Next, the replication properties of these two single-gene deleted viruses (ORFV-VEGF$^{\Delta}$-EGFP and ORFV-CBP$^{\Delta}$-EGFP) were comparatively analyzed with an equivalent reporter virus containing the wild-type genome (ORFV-WT-EGFP) in primary goat fibroblast (FB) cells.

Replication profiles of CBP$^{\Delta}$-ORFV-EGFP and VEGF$^{\Delta}$-ORFV-EGFP recombinant viruses were first evaluated using two different infection doses, including a multiplicity of infection (MOI) of 0.1 and 1 to assess the multi-step growth (Fig. 4A, C, E) and single-step growth (Fig. 4B, D, F) of these viruses, respectively. Based on the green fluorescence signal observed under microscopy, a significant decrease in infection was observed in FB cells infected with VEGF-null mutant virus throughout the infection at both MOIs, when compared to ORFV-WT-EGFP or ORFV-CBP$^{\Delta}$-EGFP (Fig. 4A, B). At 24 hpi, infection of wild-type virus at 0.1 MOI had the strongest fluorescence signal. However, the expression of the reporter gene in cells infected with CBP-null ORFV was higher than that of cells infected with wild-type ORFV at a higher MOI or at 48 hpi (Fig. 4D).

Next, the accumulated expression level of viral protein was also evaluated; western blot analysis revealed that the expression level of viral F1L protein was significantly

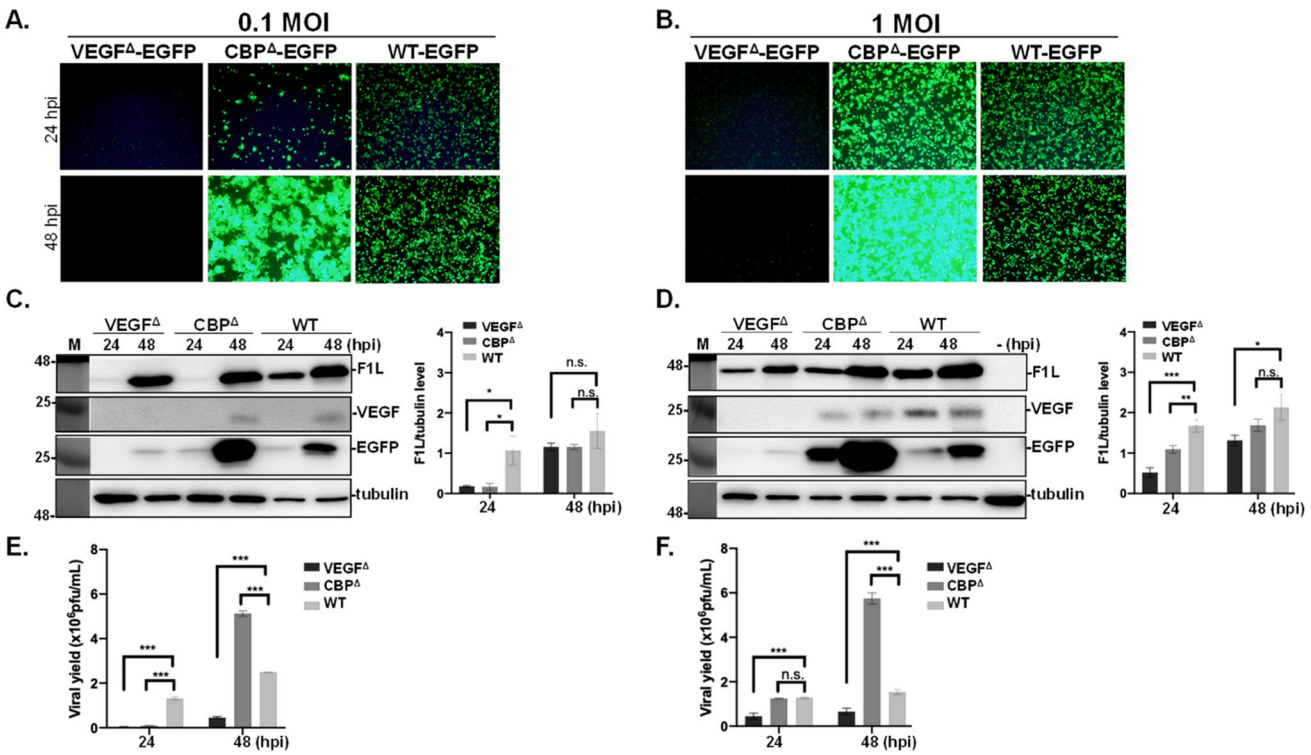

Fig. 4 Comparative characterization of the two recombinant ORFVs. FB cells were infected with the recombinant viruses at an MOI of 0.1 (**A**, **C**, **E**) or 1 (**B**, **D**, **F**) as indicated. The expression of the reporter gene was directly visualized using fluorescence microscopy (**A**). The protein expression profile (including viral proteins F1L and VEGF, the reporter GFP, and cellular tubulin) and the yield of virus progenies in cells infected with viruses for 24 and 48 hpi were determined by western blot analysis (**C**, **D**) and plaque assay (**E**, **F**), respectively. The experiments were conducted in triplicate. Bars represent the standard error of the mean. Student's *t* test was performed, and statistical differences between the mean viral F1L protein or titers between ORFV-WT-EGFP and recombinant ORFV groups were considered significant at $*p<0.05$, $**p<0.01$, and $***p<0.001$. "n.s." indicates no significance

lower in ORFV-VEGF$^{\Delta}$-EGFP and ORFV-CBP$^{\Delta}$-EGFP as compared to that expressed in WT reporter virus at 24 hpi (Fig. 4C and 4D). Nevertheless, at a later time point of infection (48 hpi), the decreased F1L expression was only significant in infection with ORFV-VEGF$^{\Delta}$-EGFP at 1 MOI, compared with ORFV-WT-EGFP (Fig. 4D). Moreover, among the three viruses analyzed, ORFV-VEGF$^{\Delta}$-EGFP had the lowest yield of viral progenies at both infection doses and time points analyzed (Fig. 4E, F), which is in accordance with the trend observed in F1L protein levels. Interestingly, in comparison to ORFV-WT-EGFP, infection with 0.1 MOI of ORFV-CBP$^{\Delta}$-EGFP yielded a significantly lower titer at 24 hpi, while viral production was drastically elevated to an extent higher than that of ORFV-WT-EGFP at 48 hpi (Fig. 4E), which is consistent with the dynamic expression level of EGFP (Fig. 4A). Collectively, the deletion of VEGF significantly affected ORFV infection, whereas the absence of the CBP gene did not compromise the ability of ORFV to replicate in the cell culture.

Pathogenesis in goats

As previously described by Mercer et al., experimental infection of sheep with WT-ORFV (NZ7 strain) by scarification of the skin generally results in discrete papules and pustules that form along the scratch line (Fleming et al. 2017). The pathogenicity of these recombinant ORFV was comparatively analyzed in a goat model, the authentic host of ORFV. In this study, following the protocol described previously (Savory et al. 2000), each of the three goats was inoculated with 10^6 pfu/0.1 mL of ORFV (i.e., ORFV-VEGF$^{\Delta}$-EGFP, ORFV-CBP$^{\Delta}$-EGFP, ORFV-WT-EGFP virus) or PBS (mock-infected control) by smearing the virus at different scratch lines. Infected skin was photographed daily to record clinical pathology, and the clinical score was determined from the appearance and size of papules and pustules that developed along the scratch line as described in the "Materials and methods." As shown in Fig. 5A, the gross pathology of the lesion in each animal infected with either the recombinant deletion virus or the wild-type virus showed no significant difference with respect to papule and pustule formation on days 4 and 7 post-infection.

To estimate the production of infectious viruses during the course of infection in goats, 1.5-mm punch biopsies were taken, and viral titers at both 7- and 10-days post-infection (dpi) were determined. Notably, the ORFV-CBP$^{\Delta}$-EGFP titers were significantly lower than those of the ORFV-WT-EGFP strain (Fig. 5C). As summarized in Table 3, compared with the ORFV-WT-EGFP virus, ORFV-CBP$^{\Delta}$-EGFP titers were reduced by as much as 14-fold and 529-fold on 7 and 10 dpi, respectively. Furthermore, the titer of ORFV-CBP$^{\Delta}$-EGFP on the skin lesions declined from 7 to 10 dpi, whereas the wild-type virus remained at a similar level during this period (Table 3). Surprisingly, the production of infectious ORFV-VEGF$^{\Delta}$-EGFP virus particles on the scarified skin was undetectable (Fig. 5B). To confirm ORFV-VEGF$^{\Delta}$-EGFP replication during the study, we extracted viral DNA from ORFV-VEGF$^{\Delta}$-EGFP-infected tissues to determine the presence of viral RNA by RT-PCR using primers targeting the viral A32L gene, a gene that is used for molecular characterization of ORFV (Chan et al. 2009). The results confirmed the presence of ORFV-VEGF$^{\Delta}$-EGFP RNA with increasing signal intensity from 4 to 10 dpi (Figure S2). Overall, these results suggested that the deletion of either CBP or VEGF significantly impaired ORFV replication relative to that of the ORFV-WT-EGFP virus in goats. Moreover, ORFV-VEGF$^{\Delta}$-EGFP infection was more attenuated than ORFV-CBP$^{\Delta}$-EGFP infection in the goat model.

Histopathology analysis of lesions in infected goats

Skin tissues of goats infected with ORFV were analyzed using H&E staining. As mentioned previously, biopsies of the ORFV-VEGF$^{\Delta}$-EGFP, ORFV-CBP$^{\Delta}$-EGFP, and ORFV-WT-EGFP viruses were obtained from the scarified skin at 4 and 10 dpi. Histological examination of skin biopsies revealed hypergranulosis (thickened cornified layer, indicated by an arrow) and increased inflammatory infiltrate, most notably within the papillary dermis (Fig. 6, cropped as a rectangle), but also invading the epidermis, which was present in all infected animals. Moreover, characteristic histological changes associated with ORFV infection, including epidermal hyperplasia and hydrophobic degeneration of keratinocytes, were observed (Fig. 6). As early as 4 dpi, animals infected with ORFV-CBP$^{\Delta}$-EGFP (Fig. 6B) showed acanthosis (thickening of the stratum basal and stratum spinosum) and orthokeratotic hyperkeratosis (thickening of the stratum corneum), as well as hydropic ballooning degeneration, representing viral infection (indicated by an arrowhead), which represents the typical WT virus infection (Fig. 6A). The same histological features were observed in ORFV-VEGF$^{\Delta}$-EGFP virus infection (Fig. 6C). However, this was not observed in the mock-infected control group (Fig. 6G). At 10 dpi, similar histopathological changes were observed, although a slight decrease in acanthosis was noted in the infected tissue samples (Fig. 6D–F). Notably, these features were not observed in the mock-infected group.

Discussion

ORFV is an ideal vector for gene delivery and heterologous gene expression (Haig and Mercer 1998; Joshi et al. 2021; Reguzova et al. 2020). Hence, the safety profile

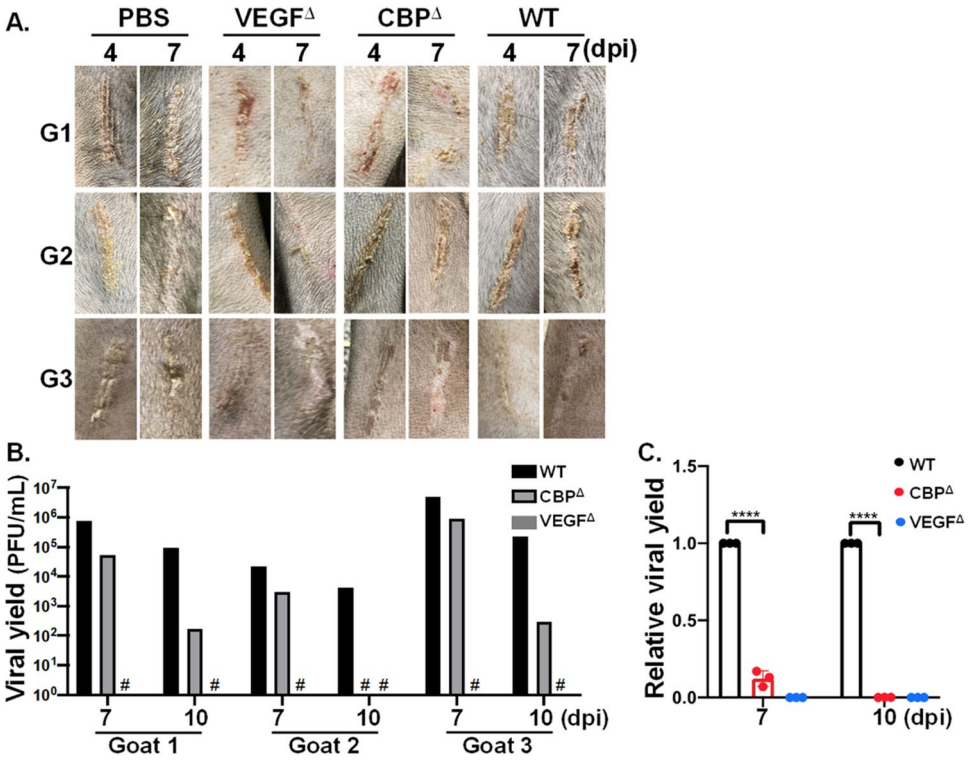

Fig. 5 Clinical course of ORFV infection in infected goats. The skin was inoculated with 10^6 pfu of ORFV-VEGF$^{\Delta}$-EGFP (VEGF$^{\Delta}$), ORFV-CBP$^{\Delta}$-EGFP (CBP.$^{\Delta}$), ORFV-WT-EGFP (WT) viruses, or PBS (mock infection). Gross pathology of ORFV lesions in goats 4 and 7 days post inoculation (dpi) (**A**). Viral production in the scarified skin of three goats infected with the three viruses at 7 and 10 dpi was measured using standard plaque assay (**B**). # indicates no virus titer. The average viral yield of defective ORFV relative to the ORFV-WT-EGFP titer in three goats was estimated and plotted (**C**). The bars represent the standard error of the mean. Student's *t* test was performed, and statistical differences between the mean titers of viral shedding in the ORFV-WT-EGFP group and recombinant ORFV groups were considered significant at $*p<0.05$, $**p<0.01$, $***p<0.001$, and $****p<0.0001$

Table 3 Viral yield was detected in the skin of the infected goats

Animal ID	dpi	Virus titer (PFU/mL)			Fold reduction[&]
		WT-EGFP	CBP$^{\Delta}$-EGFP	VEGF$^{\Delta}$-EGFP	
G1	7	7.50×10^5	5.25×10^4	ND	14.3
	10	9.25×10^4	1.75×10^2	ND	528.6
G2	7	2.25×10^4	3.0×10^3	ND	7.5
	10	4.25×10^2	ND	ND	425
G3	7	5.05×10^6	9.0×10^5	ND	5.61
	10	2.25×10^5	3.0×10^2	ND	750

ND not detected

[&]ORFV-CBP$^{\Delta}$-EGFP compared with ORFV-WT-EGFP

remains a great concern when a viral vector is used as a medical platform, particularly for therapeutic purposes. ORFV encodes several proteins that modulate host immune responses to favor viral replication, either by inhibiting or enhancing inflammatory responses (Deane et al. 2000; Haig and McInnes 2002). Given their potent immunomodulatory properties, the roles of VEGF (Savory et al. 2000) and CBP (Fleming et al. 2017) in sheep have been individually described. However, since these studies used two different viral strains circulating in New Zealand (NZ2 and NZ7), it is difficult to objectively determine the contribution of these two genes. Moreover, as per our results (Fig. 1) and the aforementioned, remarkable divergence was found in sequences of both the CBP and VEGF genes within the ORFV species; for instance, the sequence of CBP (Seet et al. 2003) or VEGF (Lyttle et al. 1994) of the NZ7 strain shares only 78% or 41% identity with that of the NZ2 strain, respectively. The similarity

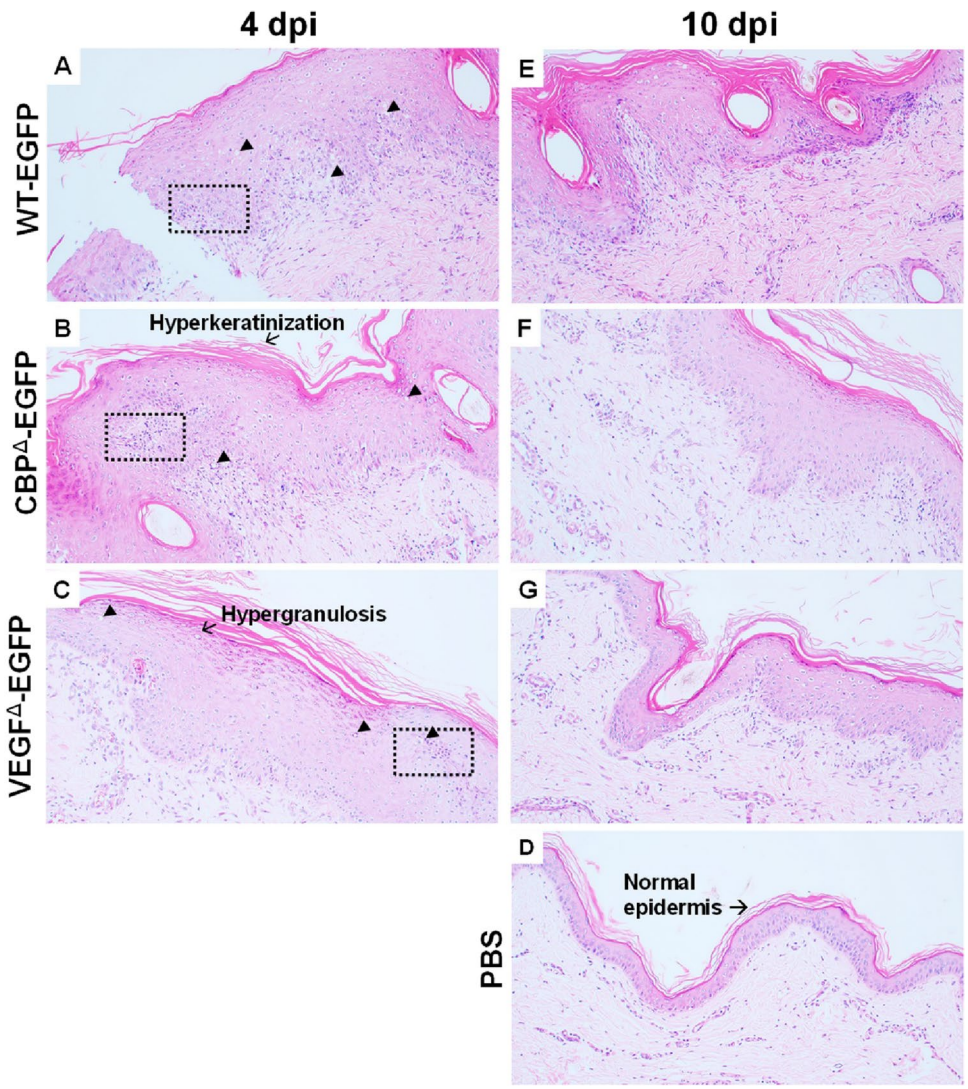

Fig. 6 Histopathology of skin biopsies of goats infected with ORFV. Histopathological examination of the ORFV-infected skin tissue. Sections from biopsy tissue infected with ORFV-WT-EGFP (**A**, **E**), ORFV-CBP$^{\Delta}$-EGFP (**B**, **F**), and ORFV-VEGF$^{\Delta}$-EGFP (**C**, **G**) at 4 and 10 dpi, or PBS-treated skin (**D**) were stained with hematoxylin and eosin (H&E stain). Typical histological features of ORFV-infected tissue, that is, dermal neutrophilic infiltration and hydropic ballooning degeneration, are indicated by dotted rectangles and arrowheads, respectively. Images were taken at 40 × magnification

of the VEGF gene between our local strain (TW/Hoping) and NZ2, the model strain used to define the function of VEGF, was 47.01%. Hence, the findings of the previous study might not be applicable to our local viral strain isolated from goats. Since the contribution of these genes to ORFV isolated from goats in Taiwan remains unknown, two null mutant orf viruses defective in the function of CBP or VEGF were generated to investigate their contribution to goat ORFV (Hoping strain) replication in vitro and pathogenesis in vivo. More importantly, the attenuation levels of these two functionally defective viruses were comparatively analyzed for the first time. The ORFV-VEGF$^{\Delta}$-EGFP virus was remarkably attenuated in both cell culture and goat models, whereas infection with the ORFV-CBP$^{\Delta}$-EGFP virus was significantly compromised only in an animal model.

The phenotype of the null mutant orf viruses established in the current study was distinct from those isolated from New Zealand in cell cultures. It has been reported that deletion of VEGF (Savory et al. 2000) or CBP (Fleming et al. 2017) did not cause viral attenuation in in vitro models. In the scenario of the VEGF-deletion virus, no discrepancy in either plaque size or growth kinetics was found between the WT and deletion virus in primary bovine testis cells (Savory et al. 2000). However, our study showed that the deletion of VEGF from ORFV (Hoping strain) led to a decrease in the size of viral plaques (Fig. 2D) and expression of the F1L viral protein (Fig. 4C, D). Importantly, a significant reduction in virus yield was observed in the ORFV-VEGF$^{\Delta}$-EGFP virus, as compared to the WT strain in goat fibroblast cells (Fig. 4E, F). Hence, the knockout of VEGF from ORFV (Hoping strain) affects viral propagation in primary cells derived from the natural host. Several factors may be involved in this inconsistent phenomenon while evaluating the function of virally encoded VEGF in cell cultures. First, the effect of VEGF may be dependent on the viral strain

or in a cell type–specific manner. Mercer et al. studied the NZ2 strain of sheep ORFV (ovORFV) on bovine testis cells (Savory et al. 2000), whereas we depicted the role of viral VEGF in goat fibroblast cells using a goat ORFV (Hoping) strain. Moreover, in a previous study (Savory et al. 2000), the viral VEGF coding region was partially removed (i.e., 116 bp) from the ovVEGFΔ-virus, whereas ORFV-VEGF$^{\Delta}$-EGFP was a VEGF-null mutant ORFV. Although VEGF-like activity, including endothelial cell mitogenesis, vascular permeability, and activation of VEGF receptor-2, has not been detected in cells infected with ovVEGFΔ, whether viral VEGF could modulate viral infection by other mechanisms has not yet been determined.

On the other hand, unlike VEGF, CBP deletion in the ORFV genome decreased viral protein expression or viral yield only at an early time point (i.e., 24 hpi) of a lower dose (that is, 0.1 MOI) of infection (Fig. 4). Surprisingly, rapid growth kinetics were observed at 48 hpi; the green fluorescence level (Fig. 4A, B) and virus yield (Fig. 4E, F) of ORFV-CBP$^{\Delta}$-EGFP significantly exceeded those of viruses harboring the WT genome. The apparent attenuation effect of CBP-knockout on viral infection suggests that the CBP gene could be non-essential for ORFV replication in vitro, which is consistent with the results of previous studies using ovORFV with CBP-knockout (CBP-ko virus) (Fleming et al. 2017; Martins et al. 2021).

It is critical to validate the phenotype of mutant viruses in models using authentic animals. The effects of CBP and VEGF on ORFV biology and pathogenesis were investigated in a goat model. ORFV infections display lesions that are typically characterized by maculopapular and proliferative scabby lesions (Fleming et al. 2017; Haig and Mercer 1998). These lesions are usually self-limiting and resolve within 4–6 weeks. However, as shown in Fig. 5A, experimental goats did not present a progressive disease course in any group after virus inoculation; the inflammation on the lesion gradually diminished after 7 dpi. In a previous study, the NZ7 strain of ovORFV that induced large pustular lesions in sheep was chosen to characterize the virulence factors of ovORFV (Fleming et al. 2017). Furthermore, the goats in the current study were approximately 8 months old, which could not be as vulnerable to ORFV infection as young kids (Hosamani et al. 2009). Hence, we suspect that the indefinite gross lesion developed by infection with the ORFV Hoping strain is possibly due to the lower virulence as compared with ovORFV used in other research groups, or due to a lower susceptibility of experimental goats.

In the sheep model, efficient replication of ovVEGFΔ was observed throughout the time of infection, although the reduced pathology of the skin lesions was evidenced by rete ridge formation (Savory et al. 2000). Intriguingly, infectious virions were not detected in ORFV-VEGF$^{\Delta}$-EGFP-infected skin samples throughout the study (Fig. 5B, C). However, to rule out the under-detectable viral production in the skin biopsies due to the failure of initial viral inoculation, virus replication was further determined by detection of viral A32L RNA using reverse transcription-PCR. As shown in Figure S2, viral RNA was readily detectable, and the increase in viral RNA levels along with the infection time indicates the progression of ORFV-VEGF$^{\Delta}$-EGFP infection. Moreover, histological examination of skin biopsies revealed characteristic histological changes associated with ORFV infection, including epidermal hyperplasia, influx of inflammatory cells, and hydrophobic degeneration of keratinocytes, indicating a bonafide infection of the ORFV-VEGF$^{\Delta}$-EGFP. Collectively, these lines of evidence endorse a severe attenuation of ORFV (Hoping strain) in the absence of VEGF. Our findings in light of the animal model are consistent with those of Savory et al., wherein the inactivation of the viral VEGF function significantly affected the pathogenesis of ORFV in its natural host (Savory et al. 2000). The virus titer in ovVEGFΔ-infected lesions was approximately 20-fold lower than that in WT, and a milder lesion (based on the formation of vascularization and rete ridge) was observed on scarified skin infected with ovVEGF-Δ (Savory et al. 2000).

According to the viral yield in the goat model, the ORFV-CBP$^{\Delta}$-EGFP virus appeared to be less attenuated than the VEGF knockout virus. ORFV-CBP$^{\Delta}$-EGFP was less pathogenic than the WT strain, as evidenced by markedly reduced virus production in the infected cells and skin tissue (Fig. 5C, Table 3). CBP deletion in the ORFV Hoping strain displayed a reduction in virus titer by approximately 14-fold and 528-fold in goats compared to ORFV-WT-EGFP at 7 and 10 dpi, respectively (Table 3). In line with the results of Martins et al., clearance of CBP-knockout ORFV was faster than that of its parental strain (Martins et al. 2021). Despite the unapparent gross pathological changes, the skin histology examination showed a typical characteristic of ORFV infection (Fig. 5). Consistent with the findings of Fleming et al. (2017) and Martins et al. (2021), this suggests that the immunomodulatory function of CBP is important for ORFV infection, disease progression, and resolution in the natural host.

In the current study, deletion of the target gene was indubitably evidenced by the absence of CBP and VEGF protein expression in immunoblot analysis (Figs. 2F and 3F), whereas the phenotype of the knockout virus was confirmed by functional assays, such as receptor binding ability and cellular activities in previous studies (Fleming et al. 2017; Savory et al. 2000). Although reduced infectivity has been well demonstrated in ovVEGFΔ virus (with partial deletion of 116 bp of OV132), or CBP-ko ORFV, in comparison to its parental strain (ovORFV), the

parameters used in those studies were not comparable to each other. Hence, the relative degree of attenuation of these recombinant viruses remains unclear. In the study of Savory et al., the attenuation of VEGF-gene deleted ORFV (ovVEGF-D) was evaluated by the formation of rete ridges, yield of virus progenies, histological comparison of infected tissues, and gross pathology, but clinical scoring in lesions was not performed (Savory et al. 2000). On the other hand, Fleming et al. (2017) highlight the attenuation of CBP-ko ORFV by estimating the clinical scores of infected skin lesions by histology analysis, the region of virus replication, and MHC-II by immunohistochemistry (IHC) assay. Following the same experimental design and based on the same criteria, this study demonstrated that ORFV-VEGF$^{\Delta}$-EGFP is less pathogenic than ORFV-CBP$^{\Delta}$-EGFP.

In conclusion, our study clearly showed that the VEGF and CBP genes are critical for the infection and virulence of ORFV (Hoping strain). Notably, recombinant ORFV defective in either VEGF or CBP expression significantly reduced viral infection; in particular, knockout of VEGF expression resulted in severe attenuation of ORFV infectivity in an animal model. As both VEGF and CBP have been clearly defined as virulence determinants for ORFV, deletion of these loci improve the overall safety of the ORFV vector platform. As evidenced in both cell culture and the natural goat host, deletion of the VEGF gene markedly reduced the yield of viral progenies, while the ability of intracellular viral propagation remained. This property renders the ORFV-VEGF$^{\Delta}$-EGFP virus an advantageous vector for the development of a live attenuated vaccine as well as for therapeutic regimens.

Supplementary Information The online version contains supplementary material available at https://doi.org/10.1007/s00253-022-12323-0.

Acknowledgements This project was supported by the Ministry of Science and Technology of Taiwan (MOST-106-2313-B-005-039-MY3 and NSTC-111-2313-B-005-043-MY3).

Author contribution WLH conceived of and designed the study. All of the authors conducted the experiments. WLH, STC, and YY analyzed the data. WLH and YY wrote the manuscript. WLH provided grants for this study. All of the authors have read and approved the manuscript.

Data availability The data generated and/or analyzed during the current study are available from the corresponding author upon reasonable request.

Declarations

Ethical statement All applicable international, national, and institutional guidelines for the care and use of animals were followed. The use of animals and experimental protocols were approved by the IACUC of the National Chung Hsing University (approval number: 110–106)

Conflict of interest The authors declare no conflicts of interest.

References

Achen MG, Jeltsch M, Kukk E, Makinen T, Vitali A, Wilks AF, Alitalo K, Stacker SA (1998) Vascular endothelial growth factor D (VEGF-D) is a ligand for the tyrosine kinases VEGF receptor 2 (Flk1) and VEGF receptor 3 (Flt4). Proc Natl Acad Sci U S A 95(2):548–553. https://doi.org/10.1073/pnas.95.2.548

Amann R, Rohde J, Wulle U, Conlee D, Raue R, Martinon O, Rziha HJ (2013) A new rabies vaccine based on a recombinant ORF virus (parapoxvirus) expressing the rabies virus glycoprotein. J Virol 87(3):1618–1630. https://doi.org/10.1128/JVI.02470-12

Byrd CM, Hruby DE (2004) Construction of recombinant vaccinia virus: cloning into the thymidine kinase locus. Methods Mol Biol 269:31–40. https://doi.org/10.1385/1-59259-789-0:031

Chan KW, Yang CH, Lin JW, Wang HC, Lin FY, Kuo ST, Wong ML, Hsu WL (2009) Phylogenetic analysis of parapoxviruses and the C-terminal heterogeneity of viral ATPase proteins. Gene 432(1–2):44–53. https://doi.org/10.1016/j.gene.2008.10.029

Chen YL, Hardman CS, Yadava K, Ogg G (2020) Innate lymphocyte mechanisms in skin diseases. Annu Rev Immunol 38:171–202. https://doi.org/10.1146/annurev-immunol-082919-093554

Chen D, Wang R, Long M, Li W, Xiao B, Deng H, Weng K, Gong D, Liu F, Luo S, Hao W (2021) Identification of in vitro and in vivo oncolytic effect in colorectal cancer cells by Orf virus strain NA1/11. Oncol Rep 45(2):535–546. https://doi.org/10.3892/or.2020.7885

Chi X, Zeng X, Li W, Hao W, Li M, Huang X, Huang Y, Rock DL, Luo S, Wang S (2015) Genome analysis of orf virus isolates from goats in the Fujian Province of southern China. Front Microbiol 6:1135. https://doi.org/10.3389/fmicb.2015.01135

Deane D, McInnes CJ, Percival A, Wood A, Thomson J, Lear A, Gilray J, Fleming S, Mercer A, Haig D (2000) Orf virus encodes a novel secreted protein inhibitor of granulocyte-macrophage colony-stimulating factor and interleukin-2. J Virol 74(3):1313–1320. https://doi.org/10.1128/jvi.74.3.1313-1320.2000

Delhon G, Tulman ER, Afonso CL, Lu Z, de la Concha-Bermejillo A, Lehmkuhl HD, Piccone ME, Kutish GF, Rock DL (2004) Genomes of the parapoxviruses ORF virus and bovine papular stomatitis virus. J Virol 78(1):168–177. https://doi.org/10.1128/jvi.78.1.168-177.2004

Eswarappa SM, Potdar AA, Koch WJ, Fan Y, Vasu K, Lindner D, Willard B, Graham LM, DiCorleto PE, Fox PL (2014) Programmed translational readthrough generates antiangiogenic VEGF-Ax. Cell 157(7):1605–1618. https://doi.org/10.1016/j.cell.2014.04.033

Feldman AT, Wolfe D (2014) Tissue processing and hematoxylin and eosin staining. Methods Mol Biol 1180:31–43. https://doi.org/10.1007/978-1-4939-1050-2_3

Fischer T, Planz O, Stitz L, Rziha HJ (2003) Novel recombinant parapoxvirus vectors induce protective humoral and cellular immunity against lethal herpesvirus challenge infection in mice. J Virol 77(17):9312–9323. https://doi.org/10.1128/jvi.77.17.9312-9323.2003

Fleming SB, McCaughan CA, Andrews AE, Nash AD, Mercer AA (1997) A homolog of interleukin-10 is encoded by the poxvirus orf virus. J Virol 71(6):4857–4861. https://doi.org/10.1128/JVI.71.6.4857-4861.1997

Fleming SB, McCaughan C, Lateef Z, Dunn A, Wise LM, Real NC, Mercer AA (2017) Deletion of the chemokine binding protein gene from the parapoxvirus Orf virus reduces virulence and pathogenesis in sheep. Front Microbiol 8:46. https://doi.org/10.3389/fmicb.2017.00046

Friebe A, Friederichs S, Scholz K, Janssen U, Scholz C, Schlapp T, Mercer A, Siegling A, Volk HD, Weber O (2011) Characterization of immunostimulatory components of orf virus (parapoxvirus ovis). J Gen Virol 92(Pt 7):1571–1584. https://doi.org/10.1099/vir.0.028894-0

Haig DM, McInnes CJ (2002) Immunity and counter-immunity during infection with the parapoxvirus orf virus. Virus Res 88(1–2):3–16. https://doi.org/10.1016/s0168-1702(02)00117-x

Haig DM, Mercer AA (1998) Ovine diseases. Orf. Vet Res 29(3–4):311–326

Hautaniemi M, Ueda N, Tuimala J, Mercer AA, Lahdenpera J, McInnes CJ (2010) The genome of pseudocowpoxvirus: comparison of a reindeer isolate and a reference strain. J Gen Virol 91(Pt 6):1560–1576. https://doi.org/10.1099/vir.0.018374-0

Heidarieh H, Hernaez B, Alcami A (2015) Immune modulation by virus-encoded secreted chemokine binding proteins. Virus Res 209:67–75. https://doi.org/10.1016/j.virusres.2015.02.028

Henkel M, Planz O, Fischer T, Stitz L, Rziha HJ (2005) Prevention of virus persistence and protection against immunopathology after Borna disease virus infection of the brain by a novel Orf virus recombinant. J Virol 79(1):314–325. https://doi.org/10.1128/JVI.79.1.314-325.2005

Hosamani M, Scagliarini A, Bhanuprakash V, McInnes CJ, Singh RK (2009) Orf: an update on current research and future perspectives. Expert Rev Anti Infect Ther 7(7):879–893. https://doi.org/10.1586/eri.09.64

Joshi LR, Knudsen D, Pineyro P, Dhakal S, Renukaradhya GJ, Diel DG (2021) Protective efficacy of an Orf virus-vector encoding the hemagglutinin and the nucleoprotein of influenza A virus in swine. Front Immunol 12:747574. https://doi.org/10.3389/fimmu.2021.747574

Lateef Z, Baird MA, Wise LM, Young S, Mercer AA, Fleming SB (2010) The chemokine-binding protein encoded by the poxvirus orf virus inhibits recruitment of dendritic cells to sites of skin inflammation and migration to peripheral lymph nodes. Cell Microbiol 12(5):665–676. https://doi.org/10.1111/j.1462-5822.2009.01425.x

Lin FY, Tseng YY, Chan KW, Kuo ST, Yang CH, Wang CY, Takasu M, Hsu WL, Wong ML (2015) Suppression of influenza virus infection by the orf virus isolated in Taiwan. J Vet Med Sci 77(9):1055–1062. https://doi.org/10.1292/jvms.14-0663

Lye L, Wang CC (1996) Thymidine kinase as a selectable marker for studying the biogenesis of glycosomes in Trypanosoma brucei. Exp Parasitol 82(2):211–217. https://doi.org/10.1006/expr.1996.0026

Lyttle DJ, Fraser KM, Fleming SB, Mercer AA, Robinson AJ (1994) Homologs of vascular endothelial growth factor are encoded by the poxvirus orf virus. J Virol 68(1):84–92. https://doi.org/10.1128/JVI.68.1.84-92.1994

Martins M, Joshi LR, Rodrigues FS, Anziliero D, Frandoloso R, Kutish GF, Rock DL, Weiblen R, Flores EF, Diel DG (2017) Immunogenicity of ORFV-based vectors expressing the rabies virus glycoprotein in livestock species. Virology 511:229–239. https://doi.org/10.1016/j.virol.2017.08.027

Martins M, Rodrigues FS, Joshi LR, Jardim JC, Flores MM, Weiblen R, Flores EF, Diel DG (2021) Orf virus ORFV112, ORFV117 and ORFV127 contribute to ORFV IA82 virulence in sheep. Vet Microbiol 257:109066. https://doi.org/10.1016/j.vetmic.2021.109066

Marzook NB, Newsome TP (2019) Construction and isolation of recombinant vaccinia virus expressing fluorescent proteins. Methods Mol Biol 2023:73–92. https://doi.org/10.1007/978-1-4939-9593-6_4

McGuire MJ, Johnston SA, Sykes KF (2012) Novel immune-modulator identified by a rapid, functional screen of the parapoxvirus ovis (Orf virus) genome. Proteome Sci 10(1):4. https://doi.org/10.1186/1477-5956-10-4

Mercer AA, Wise LM, Scagliarini A, McInnes CJ, Buttner M, Rziha HJ, McCaughan CA, Fleming SB, Ueda N, Nettleton PF (2002) Vascular endothelial growth factors encoded by Orf virus show surprising sequence variation but have a conserved, functionally relevant structure. J Gen Virol 83(Pt 11):2845–2855. https://doi.org/10.1099/0022-1317-83-11-2845

Mercer AA, Ueda N, Friederichs SM, Hofmann K, Fraser KM, Bateman T, Fleming SB (2006) Comparative analysis of genome sequences of three isolates of Orf virus reveals unexpected sequence variation. Virus Res 116(1–2):146–158. https://doi.org/10.1016/j.virusres.2005.09.011

Nash AD, Baca M, Wright C, Scotney PD (2006) The biology of vascular endothelial growth factor-B (VEGF-B). Pulm Pharmacol Ther 19(1):61–69. https://doi.org/10.1016/j.pupt.2005.02.007

Rohde J, Schirrmeier H, Granzow H, Rziha HJ (2011) A new recombinant Orf virus (ORFV, Parapoxvirus) protects rabbits against lethal infection with rabbit hemorrhagic disease virus (RHDV). Vaccine 29(49):9256–9264. https://doi.org/10.1016/j.vaccine.2011.09.121

Rohde J, Amann R, Rziha HJ (2013) New Orf virus (Parapoxvirus) recombinant expressing H5 hemagglutinin protects mice against H5N1 and H1N1 influenza A virus. Plos One 8(12):e83802. https://doi.org/10.1371/journal.pone.0083802

Rziha H, Henkel M, Cottone R, Bauer B, Auge U, Gotz F, Pfaff E, Rottgen M, Dehio C, Buttner M (2000) Generation of recombinant parapoxviruses: non-essential genes suitable for insertion and expression of foreign genes. J Biotechnol 83(1–2):137–145. https://doi.org/10.1016/s0168-1656(00)00307-2

Savory LJ, Stacker SA, Fleming SB, Niven BE, Mercer AA (2000) Viral vascular endothelial growth factor plays a critical role in orf virus infection. J Virol 74(22):10699–10706. https://doi.org/10.1128/jvi.74.22.10699-10706.2000

Seet BT, McCaughan CA, Handel TM, Mercer A, Brunetti C, McFadden G, Fleming SB (2003) Analysis of an orf virus chemokine-binding protein: shifting ligand specificities among a family of poxvirus viroceptors. Proc Natl Acad Sci U S A 100(25):15137–15142. https://doi.org/10.1073/pnas.2336648100

Sharif S, Ueda N, Nakatani Y, Wise LM, Clifton S, Lateef Z, Mercer AA, Fleming SB (2019) Chemokine-binding proteins encoded by parapoxvirus of red deer of New Zealand display evidence of gene duplication and divergence of ligand specificity. Front Microbiol 10:1421. https://doi.org/10.3389/fmicb.2019.01421

Shen Ni L, Allaudin ZN, Mohd Lila MA, Othman AM, Othman FB (2013) Selective apoptosis induction in MCF-7 cell line by truncated minimal functional region of Apoptin. BMC Cancer 13:488. https://doi.org/10.1186/1471-2407-13-488

Tan JL, Ueda N, Mercer AA, Fleming SB (2009) Investigation of orf virus structure and morphogenesis using recombinants expressing FLAG-tagged envelope structural proteins: evidence for wrapped virus particles and egress from infected cells. J Gen Virol 90(Pt 3):614–625. https://doi.org/10.1099/vir.0.005488-0

Tseng YY, Liao GR, Sen GC, Lin FY, Hsu WL (2015) Regulation of PACT-mediated protein kinase activation by the OV20.0 protein of Orf virus. J Virol 89(22):11619–29

Tseng YY, Lin FY, Cheng SF, Tscharke D, Chulakasian S, Chou CC, Liu YF, Chang WS, Wong ML, Hsu WL (2015) Functional analysis of the short isoform of orf virus protein OV20.0. J Virol 89(9):4966–79. https://doi.org/10.1128/JVI.03714-14

Voigt H, Merant C, Wienhold D, Braun A, Hutet E, Le Potier MF, Saalmuller A, Pfaff E, Buttner M (2007) Efficient priming against classical swine fever with a safe glycoprotein E2 expressing Orf virus recombinant (ORFV VrV-E2). Vaccine 25(31):5915–5926. https://doi.org/10.1016/j.vaccine.2007.05.035

Weber O, Siegling A, Friebe A, Limmer A, Schlapp T, Knolle P, Mercer A, Schaller H, Volk HD (2003) Inactivated parapoxvirus ovis (Orf virus) has antiviral activity against hepatitis B virus and herpes simplex virus. J Gen Virol 84(Pt 7):1843–1852. https://doi.org/10.1099/vir.0.19138-0

Wise LM, Veikkola T, Mercer AA, Savory LJ, Fleming SB, Caesar C, Vitali A, Makinen T, Alitalo K, Stacker SA (1999) Vascular endothelial growth factor (VEGF)-like protein from orf virus NZ2 binds to VEGFR2 and neuropilin-1. Proc Natl Acad Sci U S A 96(6):3071–3076. https://doi.org/10.1073/pnas.96.6.3071

de Castro DG, Pellizzon ACA, Braun AC, Chen MJ, Silva MLG, Fogaroli RC, Gondim GRM, Ramos H, Neto ES, Abrahao CH, Yu LS, Abdallah EA, Calsavara VF, Chinen LTD (2022) Heterogeneity of HER2 expression in circulating tumor cells of patients with breast cancer brain metastases and impact on brain disease control. Cancers (Basel) 14(13) https://doi.org/10.3390/cancers14133101

Reguzova A, Ghosh M, Muller M, Rziha HJ, Amann R (2020) Orf virus-based vaccine vector D1701-V induces strong CD8+ T cell response against the transgene but not against ORFV-derived epitopes. Vaccines (Basel) 8(2) https://doi.org/10.3390/vaccines8020295

Rintoul JL, Lemay CG, Tai LH, Stanford MM, Falls TJ, de Souza CT, Bridle BW, Daneshmand M, Ohashi PS, Wan Y, Lichty BD, Mercer AA, Auer RC, Atkins HL, Bell JC (2012) ORFV: a novel oncolytic and immune stimulating parapoxvirus therapeutic. Mol Ther 20(6):1148-57 doi:S1525-0016(16)32538-2 [pii] https://doi.org/10.1038/mt.2011.301

Wyatt LS, Earl PL, Moss B (2017) Generation of recombinant vaccinia viruses. Curr Protoc Protein Sci 89:5 13 1–5 13 18 https://doi.org/10.1002/cpps.33